MANSOURA JOURNAL OF Physics
Official Journal of Faculty of Science, Mansoura University, Egypt
E-mail: scimag@mans.edu.eg ISSN: 2974-4954

Assessing the optical characteristics of nano-composite CMC/PVP thin films embedded in green synthesized silver nanoparticles

M.elsaady [1] , A.M. Abdelghany [2] , E.Salem [1] , and A.H. Oraby [1]

[1] *Advanced Materials Research Lab., Faculty of Science, Mansoura University, 35516, Mansoura, Egypt*

[2] *Spectroscopy Department, Physics Research Institute, National Research Centre, 33 ElBehouth St., Dokki,12311,Giza, Egypt*

Received: 31/ 10 /2022
Accepted: 17 / 11 / 2022

Abstract: Nano-composite thin films comprising carboxymethyl cellulose (CMC)/ Polyvinylpyrrolidone (PVP) embedded green synthesized Silver nanoparticles (AgNPs) were successfully synthesized via the traditional solution casting route. Synthesized nanoparticles were characterized through UV/Vis., XRD, and transmission electron microscopy. Obtained data reveals the formation of cubic silver nanoparticles with surface plasmon resonance (SPR) at 420 nm and size of 70 nm that was confired by transmission electron microscopy and XRD. Synthesized samples were homogenous, transparent, and amorphous as revealed by X-ray diffraction. Prepared samples were approved to be amorphous and their optical energy gap was estimated.

keywords: PVP/CMC; Green synthesis; AgNPs; UV/Vis. spectroscopy; X-ray diffraction.

1.Introduction

In the past decade, polymer nano-composites have drawn great attention from academics due to their numerous distinctive properties compared to other materials [1-3].

Metallic nanoparticles have also been studied as a result of their large volume-to-volume surface area ratio and their unique optical, electronic, and catalytic characteristics. Polymer nano-composites comprising metallic nanoparticles find as many uses in various fields of applications utilizing water purification, catalyst, and hydrogen presser-vation. In addition; various biological models, polymers, and surfactants have been used to avoid this agglomeration activity and to stabilize and control nanoparticle structures [4, 5]. The optical absorption range of metal nanoparticles is dominated by surface plasmon resonance (SPR), which transitions to longer wavelengths as particle size increases.

The use of natural polymers in the synthesis of AgNPs has shown considerable promise for green synthetic techniques. Due to their non-toxicity and biocompatibility, natural polymers such as cellulose and its derivatives, alginates, starch, dextran, guar gums, gelatin, and others have been utilized as matrices or stabilizers in the creation of metallic nanoparticles. The backbone of biopolymers often contains several hydroxyl or carboxyl groups. There are further processes that follow the silver interaction process with functional biopolymer groups [6-8].

Due to the presence of a stiff pyrrolidone group that is high in the drawing group and is known to form a variety of complexes with other polymers, polyvinyl pyrrolidone (PVP) is an amorphous, synthetic polymer with high Tg values up to 170C. It forms films easily and has good wetting qualities in solutions. This qualifies it as an additive for paint or coatings. As a water-soluble polymer, PVP has favorable effects on protection, viscosity, absorption, solubilization, and condensation, with good solubility and biological compatibility being the most significant properties [9,10].

PVP is often non-toxic and is used in several areas, including medicine, food, cosmetics, and health care. However, difficulties in processing were caused by issues related to PVP's rigid yet delicate appearance, as well as its lack of robustness. Because of its low cytotoxicity, it is widely used in medicine. Other applications include controlled drug release technology and electrochemical devices (batteries, displays) [9].

Carboxymethyl cellulose polymer (CMC) is a biocompatible and biodegradable water-soluble polymer synthesized from natural cellulose. As a consequence, it's often used in biomedicine. For several years, it has been extensively used as a smoothing agent in fruit, and as a thickener, emulsifier, and stabilizer in various industrial and medical applications. As previously reported, CMC was used for the "green" synthesis of AgNPs as natural polymers. Cellulose ether serves as a reaction reducer and stabilizer in both situations. Clothing and medical applications may benefit from CMC hydrogels containing AgNPs [11].

The presented work aims to introduce a correlation between the structural changes resulting from the minor addition of silver nanoparticles into the amorphous polymeric network of the PVP/CMC polymer blend.

2. Sample preparation and characterization

Powdered PVP of (Mw = 40.000 g/mol) and powdered CMC of molecular weight (Mw = 250.000 g/mol) provided by Linxus co. with a ratio of 80:20 were used as a pristine source for the synthesis of the polymer blend. Silver nitrate supplied by sigma Aldrich Co. was used as received. The ethanolic mint extract was prepared using 10 g of plant leaves in 100 ml ethanol at ambient room temperature for about 2 days. The solution was then freeze-dried and used to prepare the aqueous mint extract.

Precalculated amounts of both PVP and CMC with a mass fraction of 80:20 w/w dissolved separately in double distilled water using a magnetic stirrer. Obtained viscous solutions mixed vigorously and kept at ambient room temperature for about 48h. Clear and bubble-free polymer blend solution was used for the preparation of the blend film and nanocomposite films with various mass fractions of the synthesized silver nano-particles. A constant volume of the obtained solution each time was poured into plastic Petri dishes each to ensure the formation of nearly the same thickness films. The dishes were then placed in an incubator regulated at about 50 °C for 24 h. the films were then peeled from the dishes and stored in a dry place until use. Table (1) reveals the sample nomination and composition.

Table (1) Glass nominationandcompositions**.**

Sample	PVP	CMC	AgNPs × 520 ppm
$AgNPs_0$	80	20	0
$AgNPs_1$	80	20	2
$AgNPs_2$	80	20	4
$AgNPs_3$	80	20	6
$AgNPs_4$	80	20	8
$AgNPs_5$	80	20	10

2.2 Sample Characterization

UV–Vis absorption spectra of polished parallel side samples with a constant thickness (2mm±0.1) were immediately measured in the range of 200–1000 nm using a recording double beam spectrophotometer (JASCO 570, Japan) with a spatial resolution of 1 nm. Morpho-logical characterization was obtained *via* TEM type (JEOL-JEM-2100) Japan. X-ray diffra-ction (XRD) for the studied samples was recorded via Philips PW 1710 system adopting CuKα with a wavelength of 1.5405 Å. The mean value of crystallite size (d_{size}) was estimated via Scherrer's relation:

$$d_{size} = \frac{0.9\,\lambda}{\beta\, cos\theta}$$

where λ is the X-ray wavelength and β **is** the half maximum line width.

3. Results and Discussion

3.1. Nanoparticle characterization

Using standard UV/Vis, the produced nanoparticles were studied. several researchers have reported the presence of a silver surface plasmon resonance (SPR) peak at about 420 nm as a method of using spectroscopy to confirm the production of nanosized silver [9]. Figure (1) reveals the variation of absorption intensity versus wavelength of incident radiation of the obtained solution. The spectrum shows a strong UV charge transfer absorption band around 240 nm attributed to the contamination with trace Fe^{2+} impurities that exist within the plant extract even at ppm level.

Several other shoulders and peaks at 300, 340, and 465 nm can be attributed to flavonoids, polyphenols, or other components present in the residuals of plant extract.

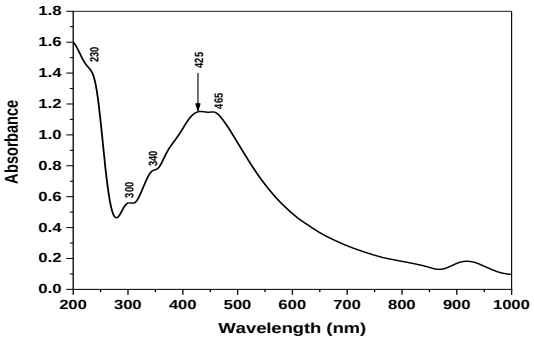

Figure (1) UV/Vis. spectral data of the studied silver nanoparticles**.**

TEM is a key tool for the direct imaging of nanomaterials and accurate quantitative assessments of the shape and estimated size of the as-prepared Ag nanoparticles. Figure (2) shows a TEM image combined with a size histogram. Obtained data reveals the formation of nano-sized silver of average size of 70 nm.

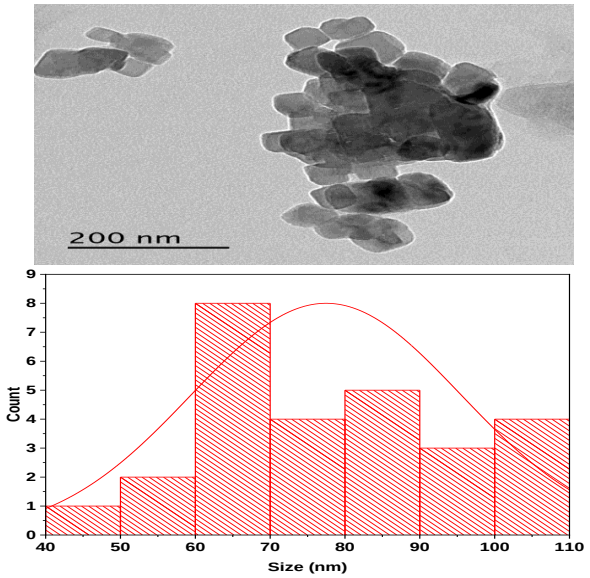

Figure (2) TEM image combined with a size histogram.

Figure (3) displays the X-ray diffraction pattern (XRD) of the green synthesized silver nanoparticles. Several sharp peaks at Bragg angles 38, 44.5, 65.5, and 78° correspond to (111), (200), (220), and (311) in agreement with that reported for the face-centered cubic (fcc) structure of silver (JCPDS file No. 04-0783) [12,13].

The X-ray diffraction profile of the synthesized silver nanoparticles is broadened as compared with that reported for bulk silver, revealing the formation of silver nanoparticles. Synthesized silver nanoparticles via reduction of silver nitrate with plant extract acts as both reducing and capping agents, Ag^{+} ions are crystalline. The crystallite size calculated using the Scherrer equation was found to range between 70-80 nm which is in agreement with that obtained from the TEM image.

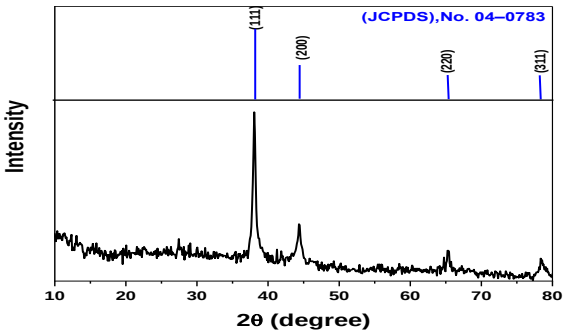

Figure (3) X-ray diffraction pattern (XRD) of the green synthesized silver nanoparticles.

3.2. UV/Visible optical absorption spectra

UV/Visible optical absorption spectral data or electronic transitions can be considered a quantitative technique that is used to measure how much a chemical substance absorbs light. This is accomplished by comparing the amount of light that passes through a sample to the amount of light that goes through a reference sample or a blank.

Figure (4) reveals the optical absorption spectral data of the studied polymeric matrices containing variable amounts of AgNP's. Obtained spectra reveal nearly the same behavior consisting of a strong absorption band located at about 220 nm within the UV range with a sharp absorption edge exactly after such a strong band. The absorption edge was also found to be shifted towards a shorter wavelength that can be correlated to the corresponding optical energy gap or transparency of the studied sample as a function of AgNPs content and without any other absorption band in the visible range till the end of measurements.

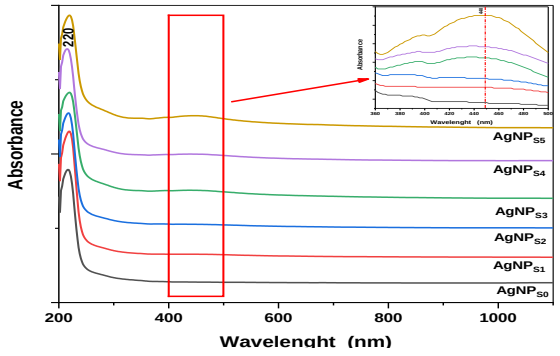

Figure (4) optical absorption spectral data of the studied polymeric nanocomposite films.

The absorption of UV or visible radiation corresponds to the excitation of outer electrons utilizing transition involving charge-transfer electrons and/or transitions of d and f electrons. Vibrations and rotations in such cases also have discrete energy levels, which can be considered as being packed on top of each electronic level.

The behavior of an electron in solids is related to the behavior of the network or compartment and the role of each component in combination with their concentration of all constituents in the polymer network [14, 15].

A specific crystal momentum (k-vector) in the Brillouin zone distinguishes the minimal-energy state in the conduction band from the maximal-energy state in the valence band. The material has an "indirect gap" if the k-vectors are different. If the crystal momentum of electrons and holes in the conduction band and the valence band are the same, the band gap is said to be "direct," and an electron can then emit a photon directly. Since the electron must pass through an intermediate state and transmit momentum to the crystal lattice, a photon cannot be released in an "indirect" gap [15].

The optical absorption process produced by electronic transitions can provide quick information about the band structure and energy gap of crystalline and amorphous materials. We determined the band gap values for an indirect and direct allowed transition of all investigated samples using the Mott and Davis [15-18] formula:

$$\alpha h\nu = B(h\nu - E_g)^r \qquad (2)$$

where B is a constant, α is the absorption coefficient, E_{opt} is the optical band gap energy, and *h* is the Plank constant.

For indirect allowed transition, $(\alpha h\nu)^{0.5}$ versus (hν), while for direct allowed transition the $(\alpha h\nu)^2$ is plotted against (hν). Figure (5, a:f) shows exemplified Tauc's plots for the energy gap values of direct and indirect allowed transition of base glass and samples containing variable amounts of AgNPs; these results are listed in Table (2).

Figure (5. a-d) reveals the variation of both direct and indirect energy gaps with the change in AgNPs content.

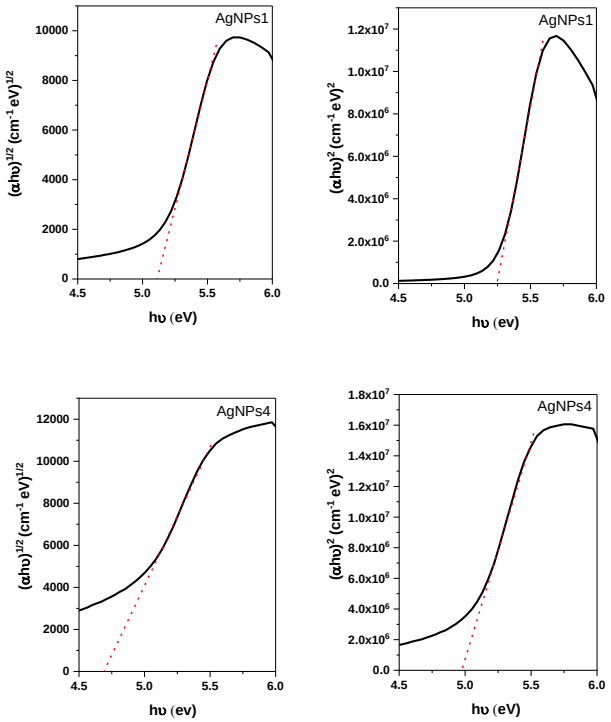

Figure (5) Tauc's plots of selected samples ($AgNP_{S1}$ and $AgNP_{S4}$).

Table (2) estimated energy gap of the studied samples.

Sample	(λg) (nm)	Eg	Eg indirect	Eg direct
		(eV)		
$AgNPs_0$	246	5.04	5.11	5.27
$AgNPs_1$	244	5.08	5.08	5.23
$AgNPs_2$	242	5.12	5.07	5.26
$AgNPs_3$	246	5.04	4.99	5.17
$AgNPs_4$	244	5.08	5.09	5.27
$AgNPs_5$	249	4.98	5.00	5.17

4. Conclusions

Green synthetic nano-composite thin films with integrated polyvinylpyrrolidone (PVP) and carboxymethyl cellulose (CMC) The conventional solution casting method was used to create silver nanoparticles with success. According to X-ray diffraction, synthesized silver nanoparticles were approved to be homogenous cubic structured with a particle size of about 70 nm. Silver nanoparticles with surface plasmon resonance (SPR) at 420 nm are permitted via UV/visible optical absorption. Using transmission electron microscopic pictures, The amorphousness of the synthesized samples was confirmed, and their optical energy gap was calculated.

5. References

1. Salahshoori, I., Seyfaee, A., & Babapoor, A. (2021). Recent advances in synthesis and applications of mixed matrix membranes. *Synthesis and Sintering*, **1(1),** 1-27.
2. Abbas, A., & Amin, H. M. (2022). Silver Nanoparticles Modified Electrodes for Electroanalysis: An Updated Review and a Perspective. *Microchemical Journal*, **175**, 107166.
3. Teepakakorn, A., & Ogawa, M. (2022). Interactions of layered clay minerals with water-soluble polymers; structural design and functions. *Applied Clay Science*, ***222***, 106487.
4. Auepattana-Aumrung, K., & Crespy, D. (2023). Self-healing and anticorrosion coatings based on responsive polymers with metal coordination bonds. *Chemical Engineering Journal*, **452**, 139055.
5. Dowek, A., Voisin, F., Le, L., Tan, C., Mallet, J. M., Carn, F., & Caudron, E. (2023). Self-assembly of gold nanoparticles by chitosan for improved epinephrine detection using a portable surface enhanced Raman scattering device. *Talanta*, **251**, 123752.
6. Palza, H. (2015). Antimicrobial polymers with metal nanoparticles. *International journal of molecular sciences*, **16(1),** 2099-2116.
7. Rao, Y. N., Banerjee, D., Datta, A., Das, S. K., Guin, R., & Saha, A. (2010). Gamma irradiation route to synthesis of highly re-dispersible natural polymer capped silver nanoparticles. *Radiation Physics and Chemistry*, **79(12),** 1240-1246.
8. Al-Shamari, A. A., Abdelghany, A. M., Alnattar, H., & Oraby, A. H. (2021). Structural and optical properties of PEO/CMC polymer blend modified with gold nanoparticles synthesized by laser ablation in water. *Journal of Materials Research and Technology*, **12**, 1597-1605.
9. Zidan, H. M., Abdelrazek, E. M., Abdelghany, A. M., & Tarabiah, A. E. (2019). Characterization and some physical studies of PVA/PVP filled with MWCNTs. *Journal of Materials Research and Technology*, **8(1),** 904-913.
10. Abdelghany, A. M., Oraby, A. H., & Farea, M. O. (2019). Influence of green synthesized gold nanoparticles on the structural, optical, electrical and dielectric properties of (PVP/SA) blend. *Physica B: Condensed Matter*, **560,** 162-173.
11. Asnag, G. M., Oraby, A. H., & Abdelghany, A. M. (2019). Green synthesis of gold nanoparticles and its effect on the optical, thermal and electrical properties of carboxymethyl cellulose. *Composites Part B: Engineering*, **172**, 436-446.
12. Ahmadpourian, A., Luna, C., Boochani, A., Arman, A., Achour, A., Rezaee, S., & Naderi, S. (2016). The effects of deposition time on surface morphology, structural, electrical and optical properties of sputtered Ag-Cu thin films. *The European Physical Journal Plus*, **131(10),** 1-7.
13. Agasti, N., & Kaushik, N. K. (2014). One pot synthesis of crystalline silver nanoparticles. *American Journal of Nanomaterials*, **2(1),** 4-7.
14. Bouabdalli, E. M., Jouad, M. E., Hajjaji, A., & Touhtouh, S. (2022). First investigation of the effect of strontium oxide on the structure of phosphate glasses using molecular dynamics simulations. *Computional Material Science*, **220**, 2023, 112068.
15. Mott, N. F. (1972). Conduction in non-crystalline systems IX. the minimum metallic conductivity. *Philosophical Magazine*, **26(4),** 1015-1026.
16. Mott, N. F., & Davis, E. A. (2012). Electronic processes in non-crystalline materials. *Oxford university press*.
17. Ikramov, R. G., Mamaxanov, A. A., Nuriddinova, M. A., Jalolov, R. M., Muminov, K. A., & Sultonov, B. Q. (2021). Calculation of the interband absorption spectra of amorphous semiconductors using the Kubo-Greenwood formula. *Journal of Applied Science and Engineering*, **25(5),** 767-772.
18. Misbah, M. H., Abdelghany, A. M., El-Agawany, F. I., Rammah, Y. S., & El-Mallawany, R. (2021). On Y_2O_3· Li_2O· Al_2O_3· B_2O_3 glasses: synthesis, structure,

physical, optical characteristics and gamma-ray shielding behavior. *Journal of Materials Science: Materials in Electronics*, **32(12**), 16242-16254.

19. Misbah, M. H., Abdelghany, A. M., El-Kemary, M., & Rammah, Y. S. (2021). Mixed modifier effect in lithium manganese metaphosphate glasses on the emission of highly dispersed Mn^{2+} centers for red - LED. *Ceramics International*, **47(22),** 32424-32432.